We are IntechOpen, the world's leading publisher of Open Access books Built by scientists, for scientists

6,900
Open access books available

186,000
International authors and editors

200M
Downloads

Our authors are among the

154
Countries delivered to

TOP 1%
most cited scientists

12.2%
Contributors from top 500 universities

WEB OF SCIENCE™

Selection of our books indexed in the Book Citation Index in Web of Science™ Core Collection (BKCI)

Interested in publishing with us?
Contact book.department@intechopen.com

Numbers displayed above are based on latest data collected.
For more information visit www.intechopen.com

Chapter

3D Ionic Networked Hydrophilic-Hydrophobic Nano Channeled Triboelectric Nanogenerators

Ravi Kumar Cheedarala

Abstract

The power demand is increasing day by day owing to the diminishing of fossil fuel reserves on the globe. To overcome the future energy crises, there is a strong need to fulfill the energy loophole by novel technologies such as triboelectric nanogenerators to harvest miniature resources from renewable natural resources. Here, I discussed the synthesis and fabrication of novel triboelectric nanogenerators (TENGs) using highly reproducible power generators as electropositive surfaces from the monomers of naphthalene tetracarboxylic dianhydride, benzdiene diamine, and sulfonated polyimide (Bno-Spi), and modified nonwoven carbon fibers (Wcf) and polytetrafluoroethylene (PTFE) and polyvinylidene difluoride (PVDF) as electronegative TENG electrodes, respectively. Here, novel double characteristic hydrophilic and hydrophobic nano-channels concerned with Bno-Spi films were proposed through contact electrification process through ion and electron transfer by an electron-donor-acceptor complex mechanism. The proposed Bno-Spi-TENG system High triboelectric open circuit voltage 75 V (Voc) and short circuit current 1 μA (Jsc) have been achieved from Bno-Spi-TENGs, in particular, and for SO_3H.Bno-Spi-TENG at 6 Hz. Besides that, we used improved knitted woven carbon fiber composite (wcf-COOH), as one of the TENGs to generate a greater open-circuit voltage (V*oc*), and short circuit current (I*sc*). Also, I aimed the contact and separation mode TENG which is using spring structure through oxidation of Wcf into Wcf-COOH followed by coupling of aniline through and one-step oxidative polymerization to get woven carbon fiber-polyaniline emraldine salt (Wcf-Pani.Es). The Wcf-PANI.Es composite film (thickness ~ 100 nm) shows the surface resistivity of 0.324 Ω m, and functions as a rubbing surface to produce charges through harvesting of energy using vertical contact-separation mode TENG. The vibrant exchanges of novel Wcf-Pani.Es, and PVDF membrane produced higher V*oc* of 95 V, and I*sc* of 180 μA, correspondingly. In specific, Wcf-Pani.Es -TENG is shown an enhancement of 498% of V*oc* concerning Wcf-COOH-TENG due to the availability of the Pani.Es layer. The novel Bno-Spi-TENGs and Wcf-Pani.Es are the potential candidates for fulfilling the need for improved energy harvesting devices as an alternate substantial choice for contact-separation mode TENGs.

Keywords: triboelectric nanogenerator, contact-electrification, Bno-Spi, Wcf-TENG, ionic electrets

1. Introduction

The urbanization process is quickening in the recent past due to speedy economic development and population growth in megalopolises considerably leads to the upsurge of resource demand, especially energy. Energy demand is gradually rising due to global warming and ecological degradation to overcome Technologists/academic scientists who are considering potential substitute energies that can desperately exchange the traditional sources for example solar, wind, and tidal energies, etc. [1–4]. Numerous kinds of energy harvesting methods were developed for accumulating energies which are thermoelectric, electromagnetic devices piezoelectric, photoelectric, electrostatic, and triboelectric devices [5, 6]. On the other hand, more robust, eco-friendly, economically viable, miniature and easy to handle, and highly reproducible energy harvesting systems with advanced technologies are desirable to satisfy the tight requirement of manufacturing demand. The energy produced from mechanical devices is a common renewable energy resource that is achieved using various modes such as humanoid motion, including the body's pulsation, and rotation, etc. [7, 8]. Freshly, triboelectric nanogenerators (TEGs) have received worldwide attention for the collecting of feasible green energy from ambient resources. Classical TEGs were designed and established based on a combination of synthetic polymers for contact and separation electrification, and electrostatic induction for generating mechanical energy [9, 10]. The appropriate choice of triboelectric paired polymers and their coherent design can upsurge the rate of energy collection and conversion efficiency [11, 12]. The oppositely charged material surfaces when they contact each other at regular intervals, consequently, the ions or electrons should be motivated to flow over the external load and, create a continuous voltage, and currents, respectively. Whiteside et al. and others have studied the ion-transfer technique by integrating ionic functional groups on the solid surface such as polystyrene (PS), glass, and silicone to produce ionic electrets on the active surface [13–19]. Microspheres with internal cross-linking's that contain mobile ions and counter ions which transfer some of them in the air through another material upon contact [20].

2. Different working mechanisms of triboelectric nanogenerators (TENGs)

Generally, TENGs produced energy by contact electrification through the coupling effect of two oppositely charged materials. While contact electrification, the dissimilar materials becomes charged after contacting each other and generate opposites triboelectric charge from the surface of two dissimilar materials with different electron affinities. When the external mechanical motion is driven, the materials were separated resulted in the potential difference between the two opposite electrodes on the backside of the resource materials. To continue the electrostatic equilibrium, the free electrons from the electrodes were flown in the external circuit to balance the induced potential difference, consequently, the mechanical energy converted into electrical energy.

Depending on the different construction strategies of potential electrodes which show four different modes of TENGs have been constructed, as explained as follows.

2.1 Vertical contact-separation style

The mechanistic approach of vertical contact-separation mode is described typically by an example. The simplest construction of TENG includes two metal

electrodes, and dielectric surface, in which two Aluminum layers work as a top electrode and bottom electrode attached to a dielectric film, respectively [21, 22]. When the mechanical system is vertically functions, the top electrode and dielectric film will be contacted each other, and therefore, the dielectric layer and electrode become positively charged, and negatively charged, respectively, owing to the triboelectrification. Once they were separated by a small detachment, the potential difference among the two electrodes could be convinced, which drive electrons to flow from the posterior-electrode to the top-electrode, subsequent in a pulse current with an external circuit coupled. If the two electrodes are brought into exchange again, the electrons will be flown back, and the current will be upturned (**Figure 1a**).

2.2 Lateral-sliding style

The basic construction of TENG in lateral sliding mode is the same as vertical contact-separation mode, but the difference is the top electrode will be moved over the bottom surface electrode as shown in **Figure 1b**. Next, the top electrode, and dielectric surface are fully overlap, and intimate interaction with each other, prominent to the oppositely charged surfaces. With the top electrode descending outward, the contact surface-area is gradually decreased until the wide-ranging departure of two surfaces. The departed surface will create a potential difference across the two TENG electrodes that generate a current movement from the upper electrode to the lower electrode. When the electrode moves backward, then there is reversed current flow to equilibrium the potential variance [23, 24]. The four fundamental methods of triboelectric nanogenerators: (a) vertical contact departure style, (b) in-plane contact-descending style, (c) single-electrode style, and (d) free standing triboelectric layer style.

2.3 Single-electrode style

The single-electrode mode TENG shows a bottom electrode is connected with the ground and the top surface is connected to the upper surface to get charged

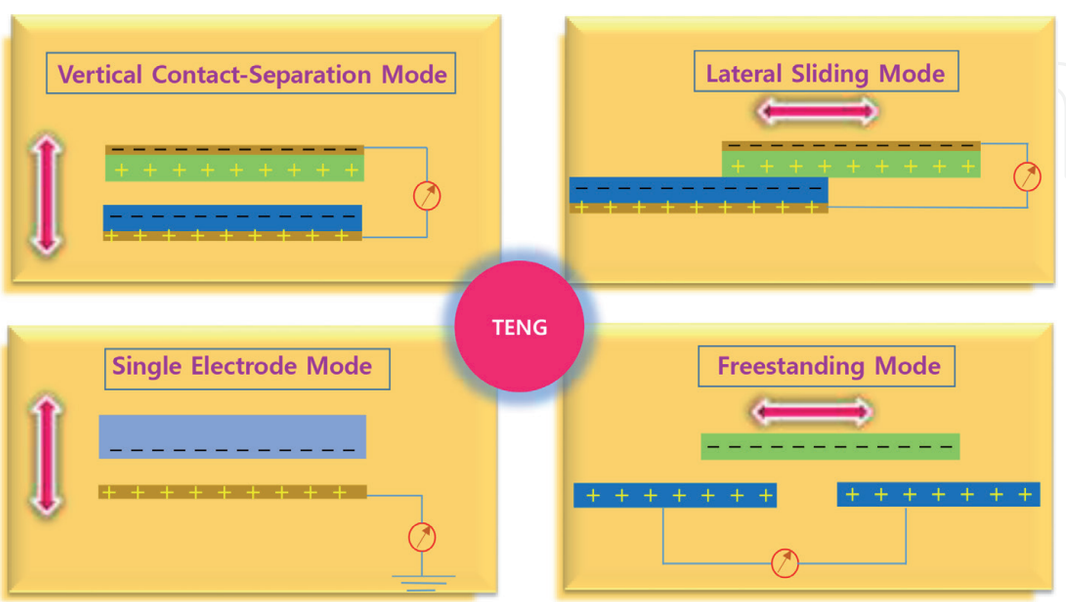

Figure 1.
The four basic triboelectric nanogenerator styles: (a) vertical contact- departure style, (b) in-plane contact-descending style, (c) single electrode style, and (d) free-standing triboelectric-layer style.

then the triboelectric effect is triggered as shown in **Figure 1c**. While approaching and leaving the top surface, the generated electric field is distributed through charged surfaces when they change. Then, the change in potential difference occurs between the bottom electrode and the ground. Subsequently, electrons can exchange between them to maintain the potential change [25, 26].

2.4 Freestanding triboelectric-layer style

Figure 1d shows the moving electrode surface which is a dielectric layer, and the two electrodes were positioned in the similar horizontal direction. The distance between the two symmetric electrodes is lesser than the length of the dielectric layer. The state of the dielectric layer and electrode are the same as in the lateral-sliding mode. Once the movement starts, simultaneously, the dielectric layer and bottom electrodes are charged oppositely as mentioned earlier. During movement the dielectric layer is sliding forward and backward, the potential difference is triggered between the two electrodes owing to the change of the affected area, and drives the electron exchanges between them [27, 28].

3. Experimental and methods of fabrication

3.1 Construction of the contact and separation mode Bno-Spi (or) Wcf-Pani.ES TENG devices

The construction and the functioning principle of the contact and separation Bno-Spi (or) Wcf-Pani.ES TENGs were discussed [20–21]. A methodical understanding of Bno-Spi (or) Wcf-Pani.ES TENGs are designated in diverse studies. Here, the building of the typical TENG models are depicted in **Figure 2**. First, the SO_3H.Bno-Spi-TENG was developed by attributing the SO_3H.Bno-Spi membrane with the sizes of 2 cm x 2 cm = 4 cm^2 on an Aluminum (Al) conductor. Next, the SO_3H.Bno-Spi-Al conductor was glued to soft sponge to reduce the reflecting strength during experiment. First, a load cell was linked to the top of the Al

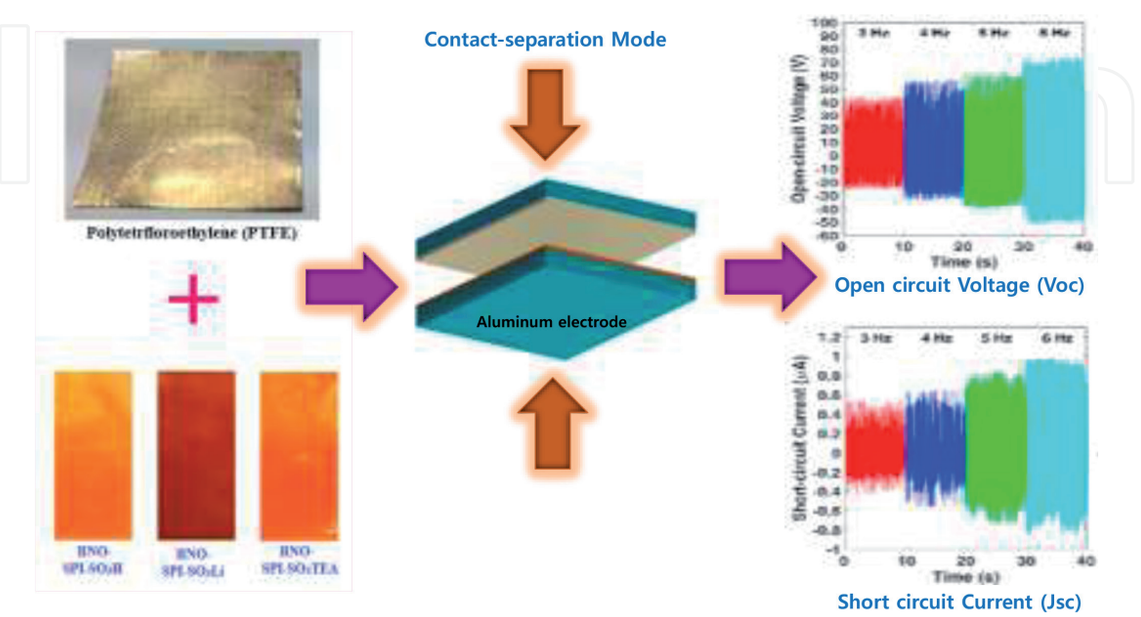

Figure 2.
Schematic illustration of a dual demonstrative Bno-Spi-TENGs aimed at robust contact electrification through vertical contact and separation style.

conductor. Secondly, the Al conductor was placed on the PTFE (or) PVDF film with similar dimensions along with soft sponge and a linear oscillator connected to a DC motor with an eccentric arrangement steadily fluctuated on a linear slider. The extreme swinging amplitude is 4 cm. The higher portion of the Bno-Spi (or) wCF-PANI.ES films (load cell, and Al) was then postponed by a cantilever style shaft of light that is connected to the linear slider. The cautious setting of the complete arrangement lead to in a slender contact between the upper and lower films while the slider oscillation is consistent. The similar protocol was followed for the all designated TENGs such as SO_3Li. Bno-Spi-Al, SO_3H.TEA.Bno-Spi-Al, and wCF-PANI.ES-Al TENGs.

4. Results and discussion

4.1 Dual demonstrative Bno-Spi-TENGs for strong contact-electrification using a vertical contact-separation approach through ions and electrons charge transfer

In this study, for the first time, we motivated to use, a Bno-Spi-TENG as a real ion, and electron-transfer route with a counter electronegative Polytetrafluoroethylene (PTFE) surface for the contact-separation electrification process [29, 30]. The anticipated novel Bno-Spi-TENG shown superior characteristics which have a special π-π stacked layer-on-layer oligomer morphology with an alternate hydrophobic and hydrophilic network with representative regular nano-channels that are comprising with -SO_3H or SO_3Li ionic electrets for active ions transfer, and inter-connected merged aromatic sextets with imides bridges for electrons transfer, respectively. The robust coordination can empower the Bno-Spi-TENG to endure the time-honored electrostatic potential on the contact surface which displays an inequality between the number of protons (cations), and electron on the targeted surface. Moreover, Bno-Spi film displays an ions hopping mechanism at hydrophilic -SO_3H or SO_3Li centers through ion charge electrets, and at the same time, the hydrophobic π-π stacking network can prompt the triboelectric open-circuit voltage Voc, and short circuit currents Jsc, individually. The induced charges on the Bno-Spi surface are comparative to its surface area and are close to the theoretical limit levied by the dielectric breakdown by air [30]. However, a noteworthy claim was shown to enhance the triboelectric polarity by fluctuating their surface morphologies, chemical construction, and interpenetration of ionic groups within the polymer network. The projected novel polymeric Bno-Spi-TENGs might show robust chemical steadiness, stretchable modulus, and strength to improve the triboelectric current [31]. The electric out-puts through altered frequencies of contact-separation manner have shown the increased Voc and Jsc of 75 V, and 1 μA at 6 Hz (**Figure 2**).

4.2 Mechanism of the dual demonstrative Bno-Spi-TENGs for strong contact-electrification through hydrophilic and hydrophobic nano-channels

In this study, for the first time, we motivated to use, a Bno-Spi-TENG is an effective ion and electron-transfer root with a counter electronegative PTFE film for the contact-separation electrification process [29, 30]. The anticipated novel Bno-Spi-TENG shown superior characteristics which have a superior π-π stacked layer-on-layer oligomeric morphology with an alternate hydrophobic and hydrophilic network with representative regular nano-channels that are comprising with -SO_3H, or SO_3Li ionic electrets for active ions transfer, and inter-connected merged

aromatic sextets with imides bridges for electrons transfer, respectively. The vigorous arrangement could allow the Bno-Spi-TENG to bear the enduring electrostatic potential on the contact surface which shows an imbalance between the numbers of electrons. For the first time, we have examined the mechanism of contact electrification procedure in two methods among the Bno-Spi films (i.e. SO_3H.Bno-Spi, SO_3Li.Bno-Spi, and SO_3H.TEA.Bno-Spi) as a positive layer, and PTFE as a negative TENG layer. At this point, the projected Bno-Spi-TENGs have been fabricated with interchanged hydrophilic, and hydrophobic nano-channels for the generation of high-throughput Voc, and Isc [32].

The mechanistic approach of sulfonic acid (SO_3H) group was attached to the backbone of Bno, during the triboelectric process, when they interact with an adjacent fluorocarbon ($-CF_2$) of PTFE polymer chain has comprised the splitting of the $-SO_3H$, or $-SO_3Li$ into positive H^+ protons or Li^+ ions, and negative SO_3^- ions. Consequently, the H^+ protons or Li^+ ions attract momentarily on the C–F to form a temporary chemical bond by the transition state of [C^+---F----- H^+ or Li^+---SO_3^-----C] to transfer the charges through an ionic mechanism between two surfaces. In certain, the charge-transfer application was approved in three steps (**Figure 3**) [33–36]. In the Step 1, the Bno-Spi, and PTFE surfaces have generated initial

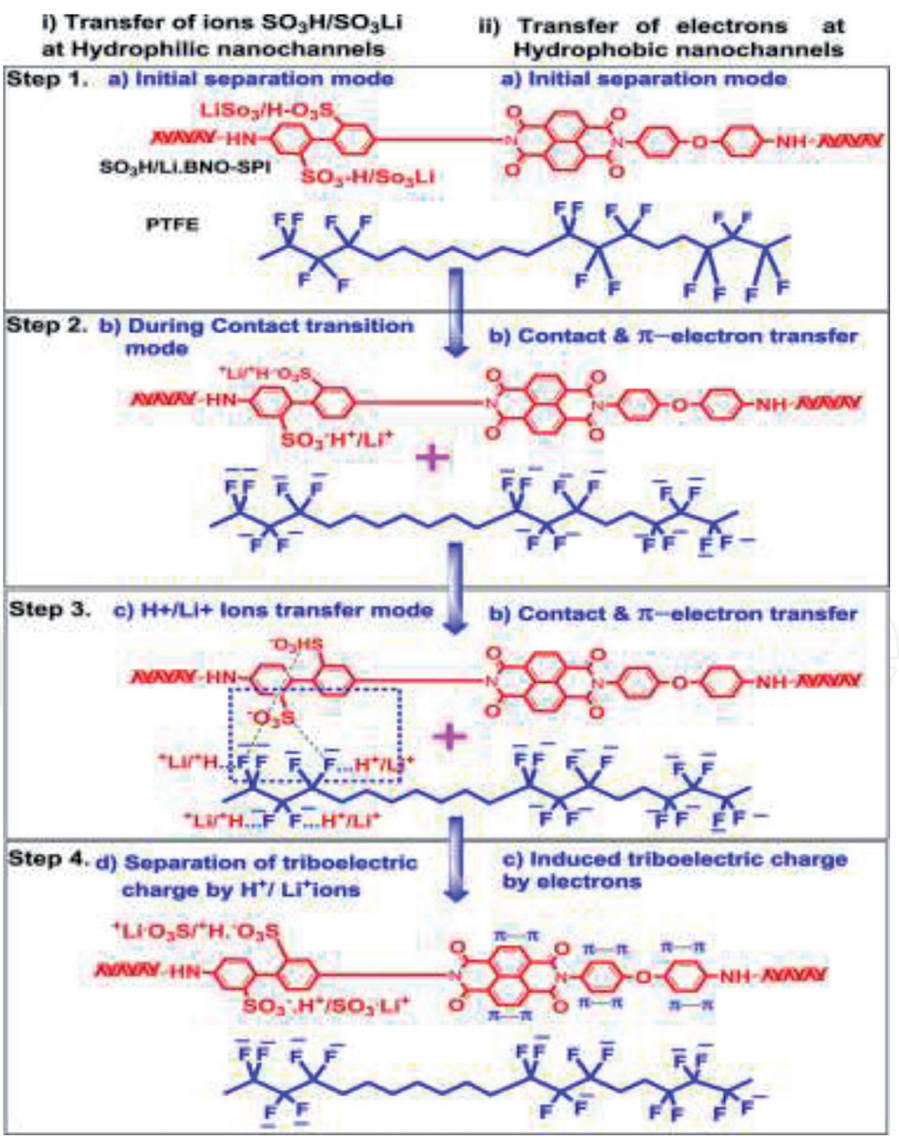

Figure 3.
The mechanistic approach of Bno-Spi-TENGs through chemical reaction pathways for the ions and electrons transfer at the hydrophilic and hydrophobic nano-channels, respectively, by contact-separation mode TENG.

charges on their surfaces where the ions from -SO_3H or -SO_3Li of the Bno-Spi, and CF_2 groups on PTFE. The Bno-Spi can produce the temporary charge-transfers through ion transfer mechanism at hydrophilic sites through nano-channels, and electron transfer at the hydrophobic nano-channels. In Step-2, when the PTFE was brought into contact, the H^+ protons or Li^+ ions were at hydrophilic nano-channels, and π-electrons at hydrophobic nano-channels of SO_3H.Bno-Spi- or SO_3Li.Bno-Spi was induced by electrostatic field effect. Thus, the projected Bno-Spi-TENG was produced electric charges through ions, and electrons from both surfaces. In Step-3, during transporting of H^+ protons or Li^+ ions from the Bno-Spi surfaces into PTFE wherein transition state, and forms a momentary ion bridge. In the four, while detaching of electrodes, the generated electric TENG charges were excited through π-π bonds in aromatic ring systems through hydrophobic nano-channels were moved into Bno-Spi-TENGs, and the net negative charges are remain the same on PTFE surface. This TENG process is continued during the contact and separation process [20].

The SO_3H.Bno-Spi-TENG, SO_3Li.Bno-Spi-TENG, and SO_3H.TEA-Bno-Spi-TENGs have shown the V*oc* and J*sc* of 75 V, and 1 μA, 43 V, and 0.6 μA, and 9 V, and 0.13 μA at applied frequency of 6 Hz, correspondingly. The V*oc,* and J*sc* of SO_3H.Bno-Spi-TENGs have shown upto 733%, and 669% concerning SO_3H.TEA-Bno-Spi-TENGs since the movement of H^+ ions remains very high on the device surface. Therefore, the maximum instantaneous power of SO_3H.Bno-Spi-TENGs, SO_3Li.Bno-Spi-TENGs, and SO_3H.TEA-Bno-Spi-TENGs were reached to 71.4 μW, 18.07 μW, and 10.89 μW at 20 MΩ conforming to the power density of 17.85 μW/cm^2 (0.1785 W/m^2), 4.515 μW/cm^2 (0.0045 W/m^2), and 2.72 μW/cm^2 (0.0272 W/m^2), correspondingly. The numerical characterization of the output performance has presented from SO_3H.Bno-Spi-TENG is 8 folds higher than SO_3H.TEA-Bno-Spi-TENG, and 1.8 folds higher than that of SO_3Li.Bno-Spi-TENG since the ion sizes were enlarged from $H^+ > Li^+ > SO_3H$.TEA. It was strongly recommended that the competence of the SO_3H.Bno-Spi-TENGs is significantly larger over the corresponding SO_3H.TEA-Bno-Spi-TENGs and SO_3Li.Bno-Spi-TENGs (**Figure 4**) [36–39].

4.3 Electric impulse spring-assisted contact separation mode TENG

In this study, we established a self-effacing and movable self-powered contact-separation approach that includes coil-aided Wcf-Pani.Es-TENG such as positive interaction superficial surface, and PVDF membrane as a negative triboelectric electrode. The established Wcf-Pani.Es-TENG presented special appearances such as inner π-π stacking's network, and amidic connections together with quaternary anilinium ions that are linking between each monomer of aniline blocks. The width, and resistivity of the Wcf-Pani.Es deposition are 0.65 μm, and 0.324 Ω which are determined by four-point probe method [21]. Owing to this morphology, the Wcf-Pani.Es is showed a huge superficial zone which is increasing the output presentation of the TENG. The established innovative Wcf-Pani.Es-TENG is revealed a short circuit current (I*sc*) of ~180 μA, and the open-circuit voltage (V*oc*) of 95 V (**Figure 5**) [40–45].

4.4 Ions transfer mechanism of contact-separation of Wcf-Pani.Es TENG

Figure 6 showed the mechanistic approach between Pani.Es and PVDF where the electric charges were reorganized when the electrification happens. During the triboelectrification process, the formation of H^+ protons from Pani.Es, and adjacent F- ions from PVDF interact to induce opposite charges. Successively, when they are in full contact mode, the H^+ ions are attracted temporarily on the C-F to form a transition bond of PVDF---F-----H^+ ---Pani.Es to transmit the charges through an

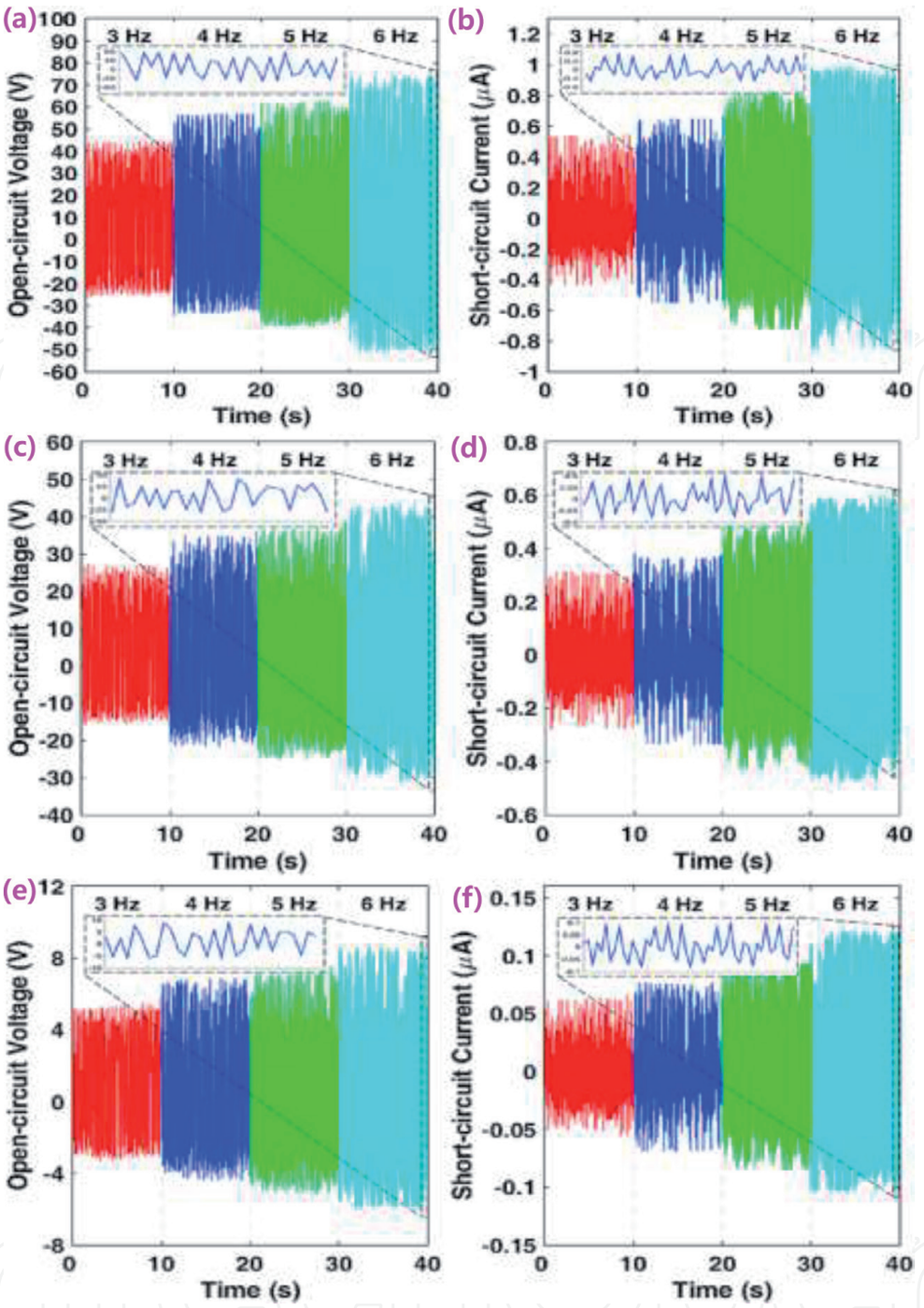

Figure 4.
(a), (c), and (e) open circuit voltages Voc and (b), (d), and (f) short-circuit currents Jsc of Bno-Spi-TENG, SO_3H.Bno-Spi-TENG, SO_3Li.Bno-Spi-TENG, and SO_3H.TEA.Bno-Spi-TENG in contradiction of PTFE film at 3 Hz, 4 Hz, 5 Hz, and 6 Hz, respectively. Inset: An enlarged view of the signals when the Bno-Spi-TENGs were interacts with PTFE surface.

ionic passage or temporary chelation between the two films [46]. The charge-transfer mechanism is carried out in four steps. Step 1, it represents the Wcf-Pani.Es, and PVDF membrane are display an early charges on their surfaces through NH^+ and F^- positioned on the Wcf-Pani.Es and PVDF, respectively. Step 2, when the PVDF membrane was carried into interaction, the H^+ protons of Wcf-Pani.Es are induced by the electrostatic field effect. Therefore, the electric charges by H^+ protons and F^- ions can generate in both films. Step 3, shows the transferring of H^+ protons is occur from the Wcf-Pani.Es surface into PVDF during the transition state, and form a temporary ion bridge between them. Step 4, during the separation process, the two oppositely charged surfaces induced a potential variance, and to minimize

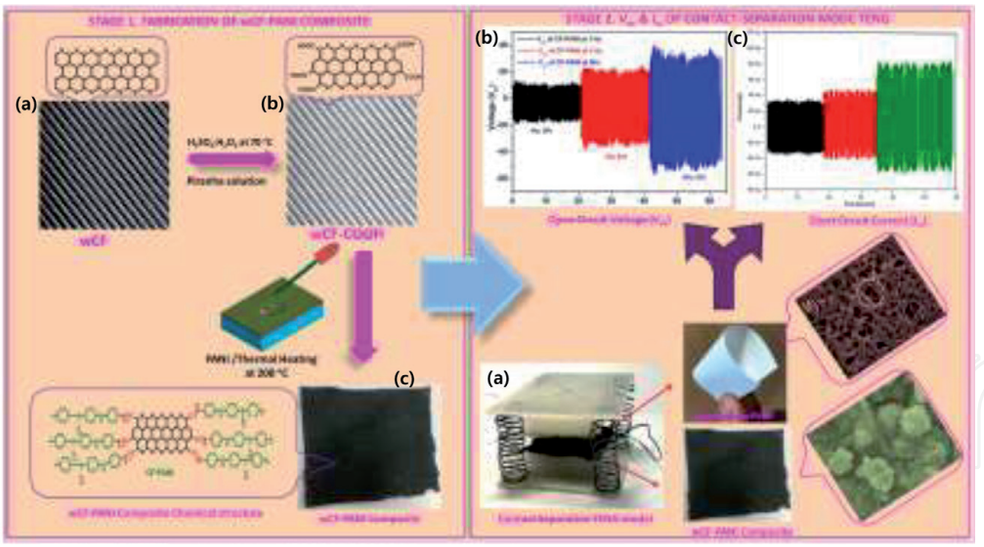

Figure 5.
Schematic illustration of electric impulse coil-aided contact separation style TENG. Stage 1. Chemical alteration of Wcf-Pani.Es film (a) woven carbon fiber mat (Wcf); b) chemically oxidized woven carbon fiber mat (Wcf-COOH); c) construction of Wcf-Pani.Es composite through electrostatic connections with aniline monomer, and in-situ oxidative polymerization using $(NH_4)_2.S_2O_8$. Stage 2. a) the actual archetypal of coil-aided TENG, (inset nanoporous PVDF membrane (upper) and variable Wcf-Pani.Es nano-pillared composite (lower) and their inset SEM pictures. b) Voc, and c) Isc.

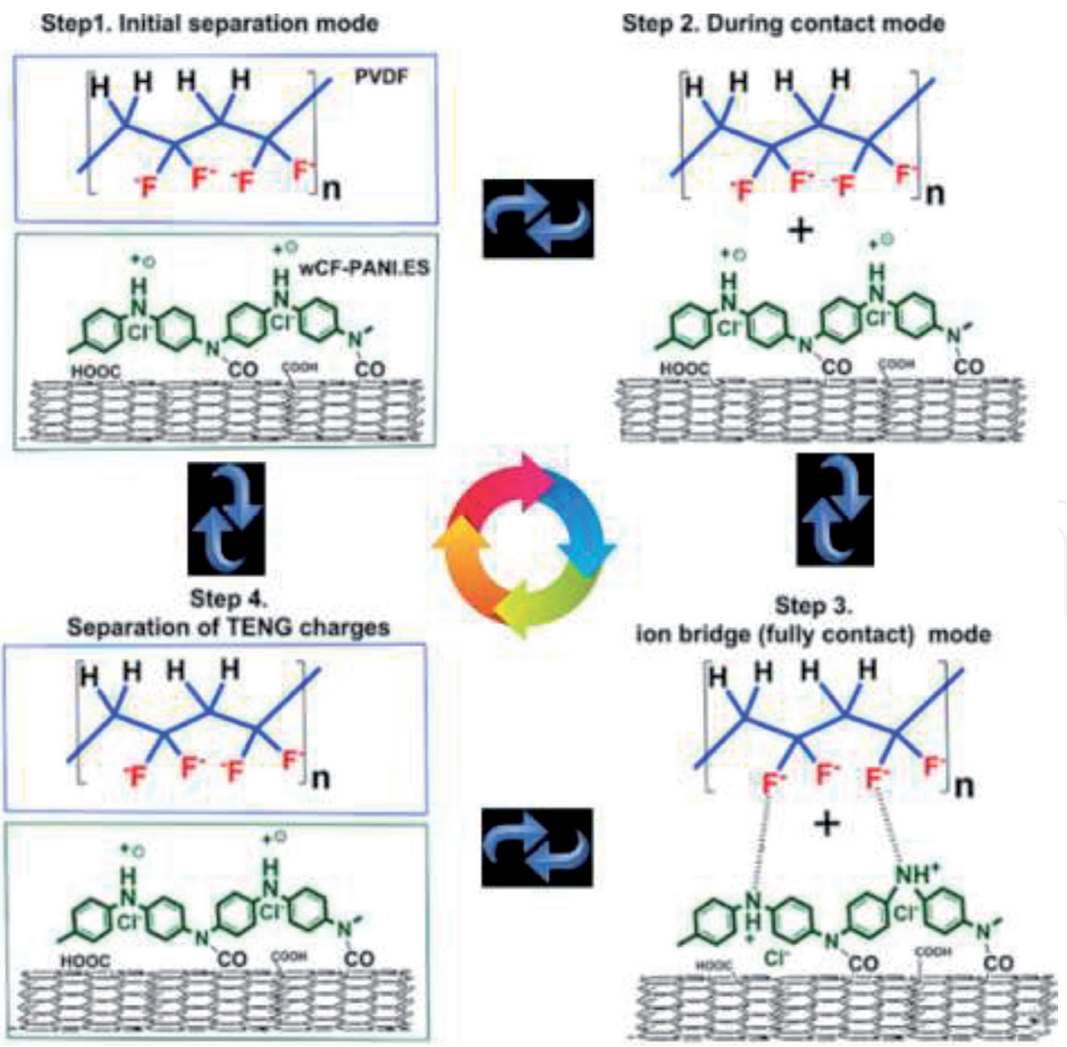

Figure 6.
The mechanism pathway of ions that are prompted between negative PVDF, and wCF-PANI.ES surfaces when they contact separated each other.

these differences, the flow of electrons emerged between two electrodes. For the validation of the automatic investigations, we achieved a measureable analysis of the out-put presentation of Wcf-Pani.Es [47–49].

4.5 Demonstration of output presentation of Wcf, Wcf-COOH, and Wcf-Pani. Es-TENGs

Initially, we inspected the performance of the Wcf, Wcf-TENG, and Wcf-COOH-TENG in contradiction of PVDF membrane through the contact-separation style technique at numerous applied regularities of 1 Hz, 3 Hz, and 5 Hz, correspondingly, is depicted in **Figure 7**. **Figure 7a** and **b** showed the V*oc,* and I*sc* of Wcf-TENG were at −2.5 V to 2.7 V, and 170 nA to −171 nA, −2.3 V to +3.1 V, and 225 nA to −221 nA, and 2.4 V to −3.7 V, and 326 nA to −328 nA at 1 Hz, 3 Hz, and 5 Hz, correspondingly, upon regular contact and separation of electrodes. Subsequently, the examination remained discovered the V*oc,* and I*sc* of Wcf-COOH-TENG have shown 3.7 V to −4.1 V, and 0.2 μA to −0.6 μA, 4.6 V to −6.4 V and 0.5 μA to −1.3 μA, and

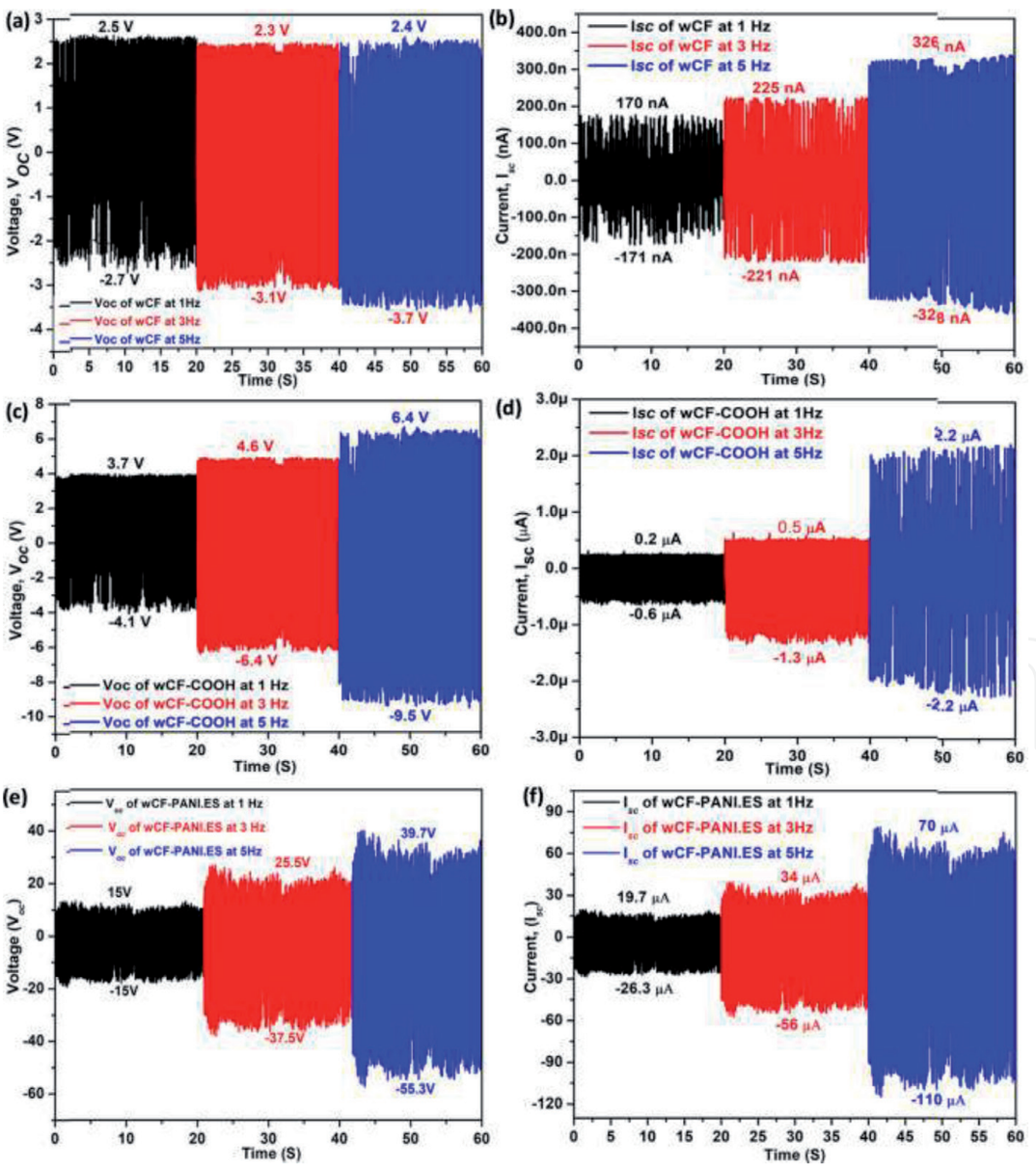

Figure 7.
The Voc, and Isc in different input circumstances in open circuit arrangements. The Voc, and Isc of (a, b) Wcf-TENG, (c, d) Wcf-COOH-TENG, and (e, f) Wcf-Pani.Es-TENG.

6.4 V to −9.5 V and 2.2 μA to −2.2 μA at 1 Hz, 3 Hz, and 5 Hz, correspondingly, as depicted in **Figure 7c** and **d**. The V*oc,* and I*sc* of Wcf-Pani.Es-TENG showed of 15 V to −15 V, and 19.7 μA to −26.3 μA, 25.5 V to −37.5 V, and 34 μA to −56 μA, and 39.7 V to −55.3 V, and 70 μA to −119 μA at 1 Hz, 3 Hz and 5 Hz, correspondingly (**Figure 7e** and **f**) [21, 50].

5. Conclusions

To develop novel technologies for the harvesting of energy, TENG is an alternative mode of technology by collecting trillions of electrons combining. These electrons are collectively obtained from various smart materials that contain high characteristic features such as flexibility, thinness and durability, long self-life, high power density, and reproducibility to harvest clean energy. Besides, TENGs can be used to transform physical characteristics such as pressure contact mode, sliding mode, and single electrode mode of features for the accumulation of energies at sub-molecular levels. Based on our novel technologies, the self-powered energy systems have given the higher out-put performance of voltage and currents. The proposed Bno-Spi-TENG and Wcf-Pani.Es-TENG are highly durable and can be used with a lower speed of contact separation modes to generate the desired amount of voltage and I*sc*. The systematic method created on the ionic electrets mechanism on the superficial electric potential of the polymeric surface has been maintained the generation of Voc and Isc from our developed novel TENGs. The established Bno-Spi-TENGs have been transported together ions, and electrons through ion, and electron transfer device when they communicated each other through PTFE. The H^+ protons or Li^+ ions attract temporarily on the C–F of PTFE surface to form a transition state of [C^+----F---- H^+ or Li^{+-}---SO_3----C] bond to transfer the charges through ionic mechanism between two active TENG films. In particular, the rate of transmission of H^+ protons, and Li^+ ions from the SO_3H.Bno-Spi-TENG, and SO_3Li. Bno-Spi-TENG surfaces have achieved huge voltage, and currents owing to the presence of the SO_3H and SO_3Li ionic clusters involved to hydrophilic nanochannels, and effective electron transfer arisen at the hydrophobic nanochannels. Also, Wcf-Pani.Es-TENG showed extraordinarily vigorous, and reliable energy gathering presentations owing to mechanically strong material assets of woven carbon fibers chemically changed by the Pani nano-flakes using a simple chemical process, this Wcf-Pani.Es-TENG has shown a great potential for self-powered TENGs even under numerous strict surroundings, and in distinct medical applications without harmful effects.

Acknowledgements

There is no funding support for this book chapter.

Conflict of interest

The authors declare no conflict of interest.

IntechOpen

IntechOpen

Author details

Ravi Kumar Cheedarala
School of Mechanical Engineering, Ulsan National Institute of Science and Technology (UNIST), Ulsan, South Korea

*Address all correspondence to: rkchidrala@gmail.com

IntechOpen

© 2021 The Author(s). Licensee IntechOpen. This chapter is distributed under the terms of the Creative Commons Attribution License (http://creativecommons.org/licenses/by/3.0), which permits unrestricted use, distribution, and reproduction in any medium, provided the original work is properly cited. CC BY

References

[1] Wiles JA, Grzybowski BA, Winkleman A, Whitesides GM. Analytical Chemistry. **2003**;**75**:4859

[2] Diaz AF, Guay J. IBM Journal of Research and Development. **1993**;**37**:249

[3] Horn RG, Smith DT, Grabbe A. Nature. **1993**;**366**:442

[4] Horn RG, Smith DT. Science. **1992**;**256**:362

[5] Fan FR, Tian ZQ, Wang ZL. Nano Energy. **2012**;**1**:328

[6] Fan FR, Lin L, Zhu G, Wu W, Zhang R, Wang ZL. Nano Letters. **2012**;**12**:3109

[7] Zhu G, Pan C, Guo W, Chen CY, Zhou Y, Yu R, et al. Nano Letters. **2012**;**12**:4960

[8] Wang S, Lin L, Wang ZL. Nano Letters. **2012**;**12**:6339

[9] Zhu G, Lin ZH, Jing Q, Bai P, Pan C, Yang Y, et al. Nano Letters. **2013**;**13**:847

[10] Lowell J, Rose-Innes AC. Advances in Physics. **1980**;**29**:9947

[11] Zhao D, Duan LT, Xue MQ, Ni W, Cao TB. Angewandte Chemie, International Edition. **2009**;**48**:6699

[12] Bandodkar AJ, Jeerapan I, Wang J. ACS Sensors. **2016**;**1**:464

[13] Soh S, Kwok SW, Liu H, Whitesides GM. Journal of the American Chemical Society. **2012**;**134**:2015

[14] Diaz AF. The Journal of Adhesion. **1998**;**67**:11

[15] Diaz AF, Alexander DF. Langmuir. **1993**;**9**:1009

[16] Liu C, Bard AJ. Nature Materials. **2008**;**7**:505

[17] McCarty LS, Winkleman A, Whitesides GM. Journal of the American Chemical Society. **2007**;**129**:4075

[18] McCarty LS, Whitesides GM. Angewandte Chemie (International Ed. in English). **2008**;**47**:2188

[19] Soh S, Liu H, Cademartiri R, Yoon HJ, Whitesides GM. Journal of the American Chemical Society. **2014**;**136**:13348

[20] Cheedarala RK, Duy LC. K. K. Ahn[a]. Nano Energy. **2018**;**44**:430

[21] Cheedarala RK, Parvez AN, Ahn KK. Nano Energy. **2018**;**53**:362

[22] B. J. Akle, M. D. Bennett, D. J. Leo, *Sen. Actuator, A* **2006**, *126*, 173.

[23] V. Panwar K. Cha, J. Park, S. Park, *Sen. Actuators, B,* **2012**, *161, 460*.

[24] Rajagopalan M, Oh IK. ACS Nano. **2011**;*5*:2248

[25] Jeon JH, Cheedarala RK, Kee CD, Oh IK. Advanced Functional Materials. **2013**;**23**:6007

[26] Cheedarala RK, Jeon JH, Kee CD, Oh IK. Advanced Functional Materials. **2014**;**25**:6005

[27] J. W. Lee, Y. T. Yoo, *Sen. Actuator, B* **2009**, *137*, 539.

[28] J. W. Lee, S. M. Hong, J. Kim, C. M. Koo, *Sen. Actuator, B* **2012**, *162*, 369.

[29] Jo C, Pugal D, Oh IK, Kim KJ, Asaka K. Progress in Polymer Science. **2013**;*38*:1037

[30] Imaizumi S, Kokubo H, Watanabe M. Macromolecules. **2013**;*45*:401

[31] Park S, An J, Suk JW, Ruoff RS. Small. **2010**;*6*:210

[32] Lee JW, Kim JH, Goo NS, Lee JY, Yoo YT. Journal of Bionic Engineering. **2010**;*7*:19

[33] C. A. Dai, C. J. Chang, A. C. Kao, W. B. Tsai, W. S. Chen, W. M. Liu, W. P. Shih, C. C. Ma, *Sensors and actuators, A* **2009**, *155*, 152.

[34] Rajagopalan M, Jeon JH, Oh IK. Sensors and Actuators B: Chemical. **2011**;*151*:198

[35] Jeon JH, Kang SP, Lee S, Oh IK. *Sensors and actuators*. B. **2009**;*143*:357

[36] Mirfakhrai T, Madden JDW, Baughman RH. Materials Today. **2007**;*10*:30

[37] Lee JW, Yu S, Hong SM, Koo CM. Journal of Materials Chemistry C. **2012**;*1*:3784

[38] Imaizumi S, Kokubo H, Watanabe M. Macromolecules. **2013**;*45*:401

[39] K. Cui, X. Feng, Y. Huang, Q. Zhao, Z. Huang, W. Zhang, *Proc. SPIE,* DOI: 10.1117/2.1200710.0901.

[40] Li J, Ma W, Song L, Niu Z, Cai L, Zeng Q, et al. Nano Letters. **2011**;*11*:4636

[41] Yoonessi M, Shi Y, Scheiman DA, Lebron-Colon M, Tigelaar DM, Weiss RA, et al. ACS Nano. **2012**;*6*:7644

[42] Pyshkina OA, Panova TV, Boeva ZA, Lezov AA, Polushina GE, Lezov AV, et al. Nanotechnologies in Russia. **2012**;*7*:629

[43] Cui K, Zheng Y, Liang J, Wang D. Nano Research. **2018**;**11**:1873

[44] Liu J, Rinzler AG, Dai H, Hafner JH, Bradley RK, Boul PJ, et al. Fuller. Pipes Sci. **1998**;**280**:1253

[45] Lu J, Kim SG, Lee S, Oh IK. Advanced Functional Materials. **2008**;*18*:1290

[46] Cheedarala RK, Song JI. RSC Advances. **2019**;**9**:31735

[47] S A Nahian, *R. K. Cheedarala,* A. N. Parvez, K. K. Ahn, Nano Energy, **2017**, 38, 447.

[48] Cheedarala RK, Kim GH, Cho S, Lee JH, Kim J, Song HK, et al. **Journal of Materials Chemistry**. **2011**;**21**:843

[49] *R. K. Cheedarala,* J. I. Song, Int. J. of Smart and Nano Materials, **2020**, 11, 38.

[50] Cheedarala RK, Song JI, Journal of Mechanics Engineering and Automation, 2019, 9, 225-229